REFINED ISOTOPE STRATIGRAPHY ACROSS THE CONTINENTAL PALEOCENE-EOCENE BOUNDARY ON POLECAT BENCH IN THE NORTHERN BIGHORN BASIN

GABRIEL J. BOWEN[1], PAUL L. KOCH[1], PHILIP D. GINGERICH[2], RICHARD D. NORRIS[3]
SANTO BAINS[4], and RICHARD M. CORFIELD[4]

[1]*Department of Earth Sciences, The University of California, Santa Cruz, California 95062*
[2]*Department of Geological Sciences and Museum of Paleontology, The University of Michigan, Ann Arbor, Michigan 48109-1079*
[3]*Woods Hole Oceanographic Institution, Woods Hole, Massachusetts 02543-1541*
[4]*Department of Earth Sciences, University of Oxford, Oxford OX1 3PR*

Abstract.— One of the most continuous and best studied continental stratigraphic sections spanning the Paleocene-Eocene boundary is preserved on Polecat Bench in the northern Bighorn Basin. The mammalian biostratigraphy of Polecat Bench sediments has been well documented, and includes a major reorganization of faunas at or near the P-E boundary. To complement the existing biostratigraphy, we measured the isotopic composition of paleosol carbonate nodules at soil-by-soil temporal resolution through the P-E boundary interval. These measurements provide a detailed record of the abrupt, transient, carbon isotope excursion that affected atmospheric and oceanic carbon reservoirs at ca. 55 million years before present [Ma]. Tests of soil thickness and diagenesis indicate that trends in the record are primary, and reflect syndepositional changes in the $\delta^{13}C$ value of atmospheric CO_2. The carbon isotope record suggests that the $\delta^{13}C$ value of atmospheric CO_2 dropped by ca. 8‰ during this interval, and then rebounded. The pattern of change is very similar to that of an independent high-resolution record of Bains et al. (submitted). Changes in the $\delta^{18}O$ of paleosol carbonates are consistent with a significant increase in local mean annual temperature during the P-E boundary event. Comparison of biotic and isotopic stratigraphies on Polecat Bench shows that faunal changes at the P-E boundary lag behind major events in the carbon and oxygen isotope records by about 10 thousand years [k.y.].

INTRODUCTION

The isotopic chemistry of authigenic soil minerals can be a sensitive recorder of climatic and environmental conditions. Authigenic carbonate from fossil soils (paleosols) is a valuable and widely used source of paleoclimatic and paleoenvironmental proxy information, and the isotope systematics of soil carbonate formation have been documented and modeled (Cerling, 1984). Fossil soils are often developed many times in a stratigraphic section and thus very useful time series can be derived from the oxygen and carbon isotope composition of paleosol carbonates, with $\delta^{18}O$ recording primarily changes in paleoclimatic variables, and $\delta^{13}C$ responding to more general paleoenvironmental shifts. Here delta values express deviations in per mil (‰) units. For example, $\delta^{18}O$ is the deviation of the oxygen isotope ratio R of a sample from that for a standard (V-PDB). This is calculated as:

$$\delta^{18}O = 1000 \times (R_{sample} - R_{standard})/R_{standard}$$

where $R = {}^{18}O/{}^{16}O$. Similarly, $\delta^{13}C$ is the deviation (in ‰) of the carbon isotope ratio of a sample from that of a standard (V-PDB), where $R = {}^{13}C/{}^{12}C$.

In: Paleocene-Eocene Stratigraphy and Biotic Change in the Bighorn and Clarks Fork Basins, Wyoming (P. D. Gingerich, ed.), *University of Michigan Papers on Paleontology,* 33: 73-88 (2001).

Extreme transient climate and carbon cycle events at the Paleocene-Eocene boundary have been documented in isotopic proxy records from a number of sources, including marine carbonates (Kennett and Stott, 1991; Zachos et al., 1993; Bains et al., 1999; Katz et al., 1999; Norris and Röhl, 1999), fossil pollen (Beerling and Jolley, 1998), and paleosol carbonates (Koch et al., 1992, 1995; Bowen et al., 2000; Bains et al., submitted). During the Paleocene-Eocene transition, marine bottom waters and high-latitude surface waters warmed dramatically (Kennett and Stott, 1991; Zachos et al., 1993), and substantial warming is indicated in terrestrial settings (Koch et al., 1995; Fricke et al., 1998). This transient climate event is associated with a large change in the carbon isotope composition of earth-surface carbon reservoirs. In the oceans, the $\delta^{13}C$ values of planktonic foraminifera dropped by ca. 2.5 to 4.5‰, while those of benthic species decreased by ca. 2.5‰ (Kennett and Stott, 1991; Zachos et al., 1993). Proxy records for atmospheric CO_2 show an abrupt decrease in $\delta^{13}C$ values of as much as 7‰ (Koch et al., 1992, 1995; Bowen et al., 2000; Cojan et al., 2000). This short-lived change in the isotopic composition of carbon at the earth's surface is best explained by the release and oxidation of at least 1500 gigatons of carbon from seafloor methane hydrate reservoirs, followed by sequestration of this excess carbon during carbon cycle re-equilibration (Dickens et al., 1997; Bains et al., 1999; Beerling, 2000).

The stratigraphic sequence on Polecat Bench in the northern Bighorn Basin of Wyoming preserves a nearly continuous series of carbonate-bearing paleosols (e.g., Fig. 1) that represent late Paleocene and early Eocene time (Gingerich, 1983). These same soils preserve fossil mammals that have been collected and studied by paleomammalogists since the late nineteenth century. Previous study of paleosol carbonates from Polecat Bench and adjacent regions of the Clarks Fork Basin indicated that the Paleocene-Eocene boundary isotope excursion is recorded as a 6 to 7‰ drop in the $\delta^{13}C$ of soil carbonate nodules (Koch et al., 1992, 1995). Here we exploit recent advances in understanding of the stratigraphy on Polecat Bench (Gingerich, this volume) to present a detailed paleosol-by-paleosol analysis of isotopic change across the Paleocene-Eocene boundary interval on Polecat Bench.

ISOTOPIC SIGNATURE OF SOIL CARBONATE

Processes that affect the isotopic composition of soil carbonate have been well documented in modern settings (Cerling, 1984; Quade et al., 1989; Cerling et al., 1991). Carbon in soil carbonate is derived from soil CO_2, which is a mixture of carbon dioxide from the atmosphere, and from organic decomposition and root respiration within the soil. The mixing of CO_2 from these sources has been modeled (Cerling, 1984; Cerling et al., 1991), and in soils with moderate to high productivity, minimal influence of atmospheric CO_2 is observed below ca. 30 cm depth. Below this depth, soil CO_2 is enriched in ^{13}C by ca. 4.4‰ relative to plant tissues and respired CO_2, due to the effects of diffusion (Cerling et al., 1991). This offset, along with consistent fractionations associated with carbonate precipitation (ca. 10.5‰) add to produce soil carbonate with a $\delta^{13}C$ value ca. 15‰ greater than that of overlying vegetation (Cerling, 1984). The isotopic composition of vegetation should track the $\delta^{13}C$ of atmospheric CO_2 with a consistent fractionation of approximately -19‰ for Paleocene-Eocene plants using a C3 photosynthetic pathway (Bocherens et al., 1993; Arens et al., 2000). Therefore, changes in the carbon isotope composition of the atmosphere are propagated and recorded in the $\delta^{13}C$ of soil carbonate CO_2.

Oxygen in soil carbonate is derived from soil water, which is derived from rain and snow (Cerling, 1984). Temporal variation in the $\delta^{18}O$ value of precipitation has commonly been interpreted to reflect variation in mean annual temperature, following the relationship developed by Dansgaard (1964). Recent work, however, has shown that this relationship is not quantitatively applicable on geological time scales (e.g., Boyle, 1997; Fricke and O'Neil, 1999). Study of modern soil carbonates has demonstrated that their oxygen isotope composition is not typically affected by rock-water interactions in the soil zone, but may reflect significant evaporative enrichment of soil waters (Quade et al., 1989).

MATERIALS AND METHODS

Fossil soil development is nearly ubiquitous within fine-grained sediments on Polecat Bench, and paleosols in this study were recognized as brown, green, orange, red, or purple mudstone horizons. Colored mudstones typically represent the B-horizons of ancient soils, and commonly contain pedogenic carbonate nodules as well as other pedogenic minerals (Bown and Kraus, 1981, 1987; Kraus, 1987). Paleosol carbonates were sampled near the base of paleosol B-horizons in freshly-exposed outcrops where there is no evidence of modern soil development (e.g., modern roots). Samples were collected at multiple stratigraphic levels within some of the thicker paleosols. Paleosols were sampled in situ in four local sections, which were mapped concurrently (Gingerich, this volume). Stratigraphic thicknesses were measured by hand leveling using a 1.5-meter Jacob's staff and by differential GPS, and detailed stratigraphic sections can be found elsewhere in this volume. Local sections were correlated by tracing marker beds (Gingerich, this volume), and results are presented on a composite stratigraphic scale. A similar record, generated independently, is presented in Bains et al. (submitted).

In the laboratory, carbonate nodules were polished flat on a lapidary wheel using 600-grit silica carbide powder, washed, then dried in a low temperature oven. Samples (ca. 100 μg) were drilled from the polished surfaces under a binocular microscope using a mounted dental drill. Primary micritic carbonate and secondary diagenetic spar were sampled independently, and, where possible, two samples were drilled from each of two nodules from every soil in each local section. Samples were roasted *in vacuo* at 400° C for 1 hour to remove organic contaminants. These were analyzed using a Micromass Optima or Prism gas-source mass spectrometer, following reaction with 100% phosphoric acid at 90° C, with the aid of an

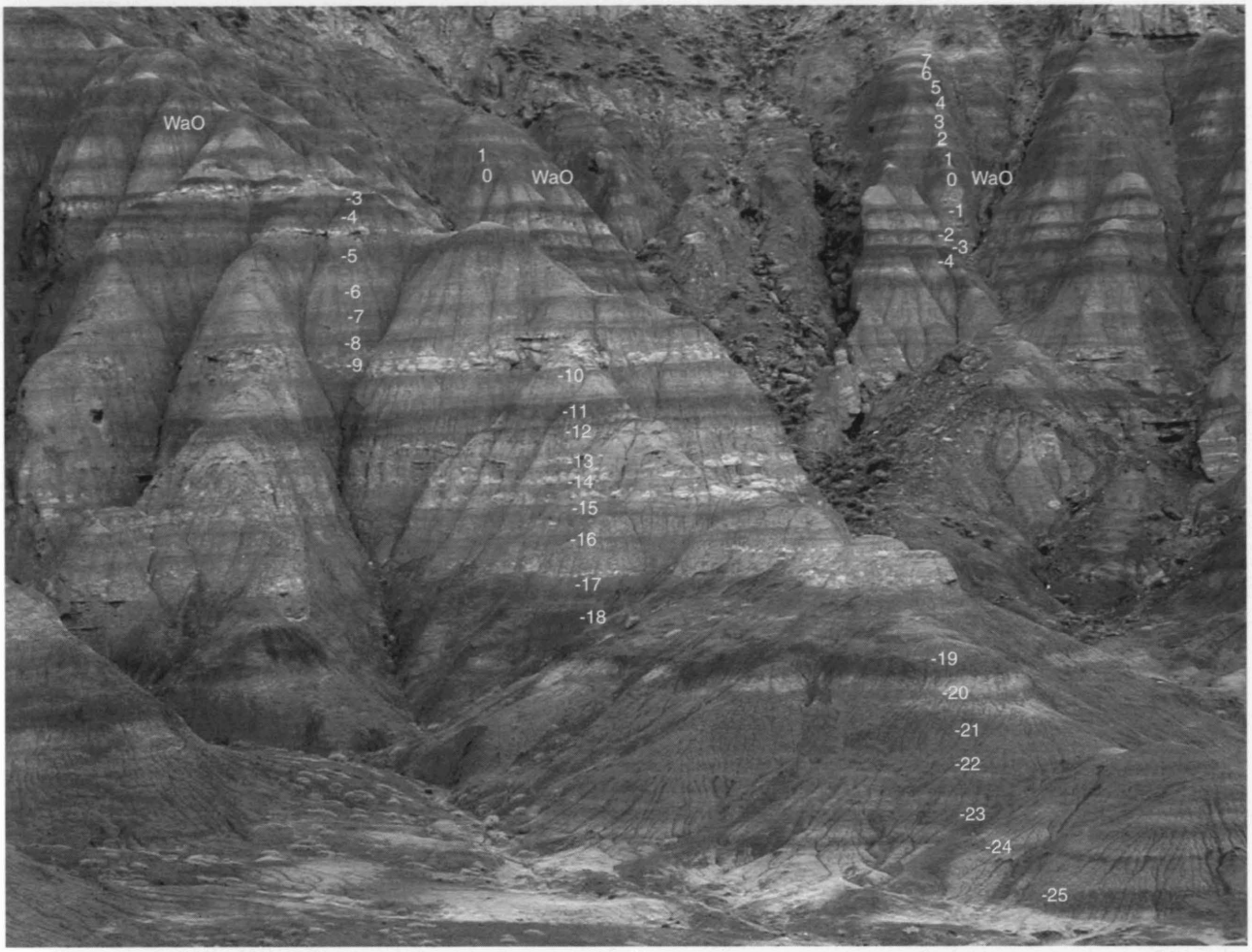

FIGURE 1 — Orange, red, and purple paleosol horizons (numbered darker bands) at the base of the carbon isotope excursion on Polecat Bench (Bains and Norris numbering system is shown here). Principal marker beds of Gingerich (Gingerich, this volume: figs. 7 and 8) are equivalent to beds numbered here, as follows: Thick Orange = beds -23 through -21; Purplish red mudstone = bed -19; Red mudstones = bed -11; Purple-0 = bed -5; Top Brown = bed -1; Lower Double-Red A and B = beds 0 and 1; and Purple-2 = bed 4. The carbon isotope excursion begins at the thin red mudstone represented by bed -8 here. University of Michigan vertebrate locality SC-404 with *Meniscotherium priscum* is at the level of beds -3 and -4. The Wa-0 faunal zone begins at bed 0. In this section the top of Wa-0 and the top of the carbon isotope excursion are missing due to truncated by the scour-and-fill sequence starting above bed 7.

automated Isocarb device. Analytical precision, based on repeated analysis of an in-house standard, was better than 0.1‰ for both carbon and oxygen.

RESULTS

Carbon and oxygen isotope measurements of micrite sampled from Polecat Bench paleosol are listed in Table 1. Ancillary measurements of the thickness of the B-horizons from which soil carbonates were collected are listed in Table 2. In addition, analyses of diagenetic spar from 10 carbonate nodules are presented in Table 3.

Within-Soil Variation and Variation through Time

A minimum of 57 distinct soils are represented in this study, spanning ca. 115 meters of stratigraphic section. The measured carbon isotope compositions span a range of -16.7‰ to -7.2‰, while $\delta^{18}O$ values were between -17.5‰ and -7.4‰. Both are plotted by stratigraphic level in Figure 2. These data show fairly tight grouping (total range of ca. 1 to 3‰) of carbon and oxygen isotope values at most stratigrapic levels. Notable exceptions occur at the base of the composite section, and at the 1519 m level (carbon and oxygen) and 1544 m level (oxygen). Also apparent is a distinct stratigraphic interval

TABLE 1 — Carbon and oxygen isotope values of micritic carbonate from the Paleocene-Eocene boundary interval on Polecat Bench. Samples in italics were culled and not used in interpretation of $\delta^{13}C$ excursion.

Soil	Sample	Level	$\delta^{13}C$	$\delta^{18}O$	Soil	Sample	Level	$\delta^{13}C$	$\delta^{18}O$
PB-00-04-16	1A	1594.2	-8.1	-8.3	PB-00-02-14	2A	1537.0	-12.8	-9.1
PB-00-04-16	1B	1594.2	-8.7	-8.6	PB-00-02-14	2B	1537.0	-12.5	-9.4
PB-00-04-16	2A	1594.2	-9.3	-8.4	PB-00-02-13	1A	1534.8	-13.3	-8.1
PB-00-04-16	2B	1594.2	-9.3	-8.3	PB-00-02-13	1B	1534.8	-13.2	-8.2
PB-00-04-15	1A	1584.7	-8.8	-8.4	PB-00-02-12	12A-1A	1533.5	-14.3	-10.0
PB-00-04-15	1B	1584.7	-8.5	-8.3	PB-00-02-12	12A-1B	1533.5	-14.1	-9.3
PB-00-04-15	2A	1584.7	-8.7	-8.4	PB-00-02-12	12A-2A	1533.5	-14.2	-9.4
PB-00-04-15	2B	1584.7	-8.7	-8.4	PB-00-02-12	12A-2B	1533.5	-14.2	-9.4
PB-00-04-14	1A	1574.7	-8.9	-9.2	PB-00-02-12	12B-1A	1533.0	-12.9	-8.8
PB-00-04-14	1B	1574.7	-8.7	-8.6	PB-00-02-12	12B-1B	1533.0	-13.2	-8.6
PB-00-04-14	2A	1574.7	-9.2	-8.8	PB-00-02-12	12B-2A	1533.0	-12.3	-8.9
PB-00-04-14	2B	1574.7	-8.3	-8.5	PB-00-02-12	12B-2B	1533.0	-12.5	-9.1
PB-00-04-13	1A	1572.8	-8.5	-9.3	PB-00-02-11	1A	1532.2	-13.8	-8.0
PB-00-04-13	1B	1572.8	-8.9	-8.9	*PB-00-02-11*	*1B*	*1532.2*	*-14.5*	*-9.8*
PB-00-04-13	2A	1572.8	-9.2	-9.4	PB-00-02-11	1C	1532.2	-13.7	-7.9
PB-00-04-13	2B	1572.8	-8.7	-8.7	PB-00-02-11	2A	1532.2	-13.8	-8.0
PB-00-04-12	1A	1568.6	-9.1	-8.7	PB-00-02-11	2B	1532.2	-13.8	-8.2
PB-00-04-12	1B	1568.6	-9.3	-8.7	PB-00-02-10	1A	1531.6	-13.9	-8.0
PB-00-04-12	2A	1568.6	-7.2	-9.4	PB-00-02-10	1B	1531.6	-13.7	-8.2
PB-00-04-12	2B	1568.6	-7.7	-9.3	PB-00-02-10	2A	1531.6	-13.8	-8.2
PB-00-04-11	1A	1568.2	-9.0	-9.0	PB-00-02-10	2B	1531.6	-14.0	-8.1
PB-00-04-11	1C	1568.2	-8.8	-8.2	PB-00-02-09U	1A	1531.0	-13.9	-8.9
PB-00-04-11	2B	1568.2	-9.1	-8.3	PB-00-02-09U	1B	1531.0	-13.9	-8.8
PB-00-04-11	2C	1568.2	-9.2	-7.8	PB-00-02-09U	2A	1531.0	-13.4	-8.8
PB-00-04-10	1A	1562.4	-9.9	-8.2	PB-00-02-09U	2B	1531.0	-13.8	-8.9
PB-00-04-10	1B	1562.4	-8.9	-8.2	PB-00-02-09	1A	1530.5	-13.6	-9.2
PB-00-04-10	2A	1562.4	-8.9	-7.9	PB-00-02-09	1B	1530.5	-13.7	-8.7
PB-00-04-10	2B	1562.4	-9.6	-8.7	PB-00-02-09	2A	1530.5	-13.7	-9.5
PB-00-04-09	1A	1559.5	-8.7	-9.0	*PB-00-02-09*	*2B*	*1530.5*	*-12.9*	*-10.7*
PB-00-04-09	1B	1559.5	-8.8	-9.1	PB-00-02-09	2C	1530.5	-12.7	-8.4
PB-00-04-09	2A	1559.5	-7.4	-9.2	PB-00-02-08	1A	1529.1	-13.9	-9.1
PB-00-04-09	2B	1559.5	-7.2	-8.9	PB-00-02-08	1B	1529.1	-13.7	-9.0
PB-00-02-23	1A	1559.4	-9.4	-8.7	PB-00-02-08	2A	1529.1	-13.8	-8.3
PB-00-02-23	1B	1559.4	-9.4	-8.6	PB-00-02-08	2B	1529.1	-13.9	-8.4
PB-00-02-23	2A	1559.4	-8.2	-9.0	PB-00-02-07	07A-1A	1528.5	-12.8	-9.6
PB-00-02-23	2B	1559.4	-8.3	-9.2	PB-00-02-07	07A-1B	1528.5	-12.4	-9.8
PB-00-04-08	1A	1558.6	-9.1	-8.4	PB-00-02-07	07A-2A	1528.5	-13.1	-8.8
PB-00-04-08	1B	1558.6	-9.5	-9.8	PB-00-02-07	07A-2B	1528.5	-13.1	-9.1
PB-00-04-08	2A	1558.6	-8.4	-9.7	PB-00-02-07	07B-1A	1528.0	-13.4	-8.4
PB-00-04-08	2B	1558.6	-8.2	-9.5	PB-00-02-07	07B-1B	1528.0	-13.6	-8.4
PB-00-04-06	1A	1554.3	-9.3	-8.4	PB-00-02-07	07B-2A	1528.0	-12.4	-8.7
PB-00-04-06	1B	1554.3	-9.1	-8.3	*PB-00-02-07*	*07B-2B*	*1528.0*	*-12.4*	*-10.5*
PB-00-02-22	1A	1554.2	-9.2	-9.0	PB-00-02-07	07B-2C	1528.0	-12.6	-8.2
PB-00-02-22	1B	1554.2	-8.8	-8.9	PB-00-02-07	07C-1A	1527.0	-13.5	-8.3
PB-00-02-22	2A	1554.2	-9.6	-9.3	PB-00-02-07	07C-1B	1527.0	-13.5	-8.2
PB-00-02-22	2B	1554.2	-8.8	-8.9	PB-00-02-07	07C-2A	1527.0	-13.5	-8.2
PB-00-04-05	1A	1553.7	-9.2	-8.7	PB-00-02-07	07C-2B	1527.0	-14.2	-8.5
PB-00-04-05	1B	1553.7	-8.9	-8.5	PB-00-02-07	07D-1A	1526.3	-14.3	-8.6
PB-00-04-05	2A	1553.7	-9.5	-8.5	PB-00-02-07	07D-1B	1526.3	-14.3	-8.8
PB-00-04-05	2B	1553.7	-9.5	-8.9	PB-00-02-07	07D-2A	1526.3	-14.5	-8.7
PB-00-04-04	1A	1549.5	-9.6	-9.3	PB-00-02-07	07D-2B	1526.3	-14.4	-8.8
PB-00-04-04	1B	1549.5	-9.9	-9.1	PB-00-02-06	1A	1525.3	-13.2	-9.0
PB-00-04-04	2A	1549.5	-9.9	-8.4	PB-00-02-06	1B	1525.3	-12.8	-8.9
PB-00-04-04	2B	1549.5	-9.9	-9.3	PB-00-02-06	2A	1525.3	-14.0	-8.9
PB-00-02-21	1A	1549.0	-9.7	-10.1	PB-00-02-06	2B	1525.3	-14.4	-8.4
PB-00-02-21	1B	1549.0	-9.7	-9.8	PB-00-02-05	1A	1524.2	-14.0	-8.8
PB-00-02-21	2B	1549.0	-9.6	-9.7	PB-00-02-05	1B	1524.2	-13.7	-8.6
PB-00-02-21	2C	1549.0	-9.7	-8.9	PB-00-02-05	2A	1524.2	-13.9	-8.9
PB-00-04-03	1A	1548.4	-9.8	-8.6	PB-00-02-05	2B	1524.2	-13.9	-8.8
PB-00-04-03	1B	1548.4	-9.9	-8.4	PB-00-02-04	1A	1523.8	-15.6	-8.0
PB-00-04-03	2A	1548.4	-9.9	-8.5	PB-00-02-04	1B	1523.8	-13.9	-8.2
PB-00-04-03	2B	1548.4	-9.9	-8.4	PB-00-02-04	2A	1523.8	-14.0	-8.3
PB-00-02-20	1A	1547.2	-9.5	-9.6	PB-00-02-04	2B	1523.8	-14.0	-8.2
PB-00-02-20	1B	1547.2	-9.6	-9.6	PB-00-02-03	1A	1522.9	-14.2	-7.9
PB-00-02-20	2A	1547.2	-9.8	-9.7	PB-00-02-03	1B	1522.9	-14.3	-7.8
PB-00-02-20	2B	1547.2	-9.8	-9.7	PB-00-02-03	2A	1522.9	-14.1	-8.0
PB-00-02-19	1A	1545.1	-10.1	-8.7	PB-00-02-03	2B	1522.9	-14.2	-8.1
PB-00-02-19	1B	1545.1	-9.7	-8.8	PB-00-01-15	15A-1A	1521.9	-13.3	-7.8
PB-00-02-19	2A	1545.1	-10.4	-9.4	PB-00-01-15	15A-1B	1521.9	-13.4	-7.6
PB-00-02-19	2B	1545.1	-10.2	-9.3	PB-00-01-15	15B-1A	1521.2	-13.7	-8.3
PB-00-04-02	*1A*	*1544.5*	*-11.5*	*-15.9*	PB-00-01-15	15B-1B	1521.2	-13.8	-8.5
PB-00-04-02	*1B*	*1544.5*	*-10.7*	*-17.2*	PB-00-01-15	15B-2A	1521.2	-14.3	-8.3
PB-00-04-02	*2A*	*1544.5*	*-11.5*	*-17.4*	PB-00-01-15	15B-2B	1521.2	-14.3	-8.1
PB-00-04-02	*2B*	*1544.5*	*-11.4*	*-17.5*	PB-00-02-02	1A	1520.5	-13.8	-7.8
PB-00-02-18	1A	1543.9	-10.2	-9.3	PB-00-02-02	1B	1520.5	-13.7	-7.9
PB-00-02-18	1B	1543.9	-10.1	-8.9	PB-00-02-02	2A	1520.5	-13.7	-8.0
PB-00-02-18	2A	1543.9	-10.2	-9.1	PB-00-02-02	2B	1520.5	-13.1	-8.3
PB-00-02-18	2B	1543.9	-10.2	-9.3	PB-00-01-14	14A-1A	1519.7	-13.9	-8.3
PB-00-02-17	1A	1543.0	-10.3	-8.7	PB-00-01-14	14A-1B	1519.7	-13.9	-8.6
PB-00-02-17	1B	1543.0	-10.1	-8.4	*PB-00-01-14*	*14A-2A*	*1519.7*	*-12.9*	*-9.9*
PB-00-02-17	2A	1543.0	-11.2	-8.6	*PB-00-01-14*	*14A-2B*	*1519.7*	*-13.1*	*-9.9*
PB-00-02-17	2B	1543.0	-10.9	-8.1	*PB-00-01-14*	*14B-1A*	*1519.3*	*-13.7*	*-10.2*
PB-00-04-01	1A	1541.0	-10.6	-8.5	*PB-00-01-14*	*14B-1B*	*1519.3*	*-12.0*	*-13.5*
PB-00-04-01	1B	1541.0	-10.6	-8.5	*PB-00-01-14*	*14B-2A*	*1519.3*	*-11.4*	*-15.0*
PB-00-04-01	2A	1541.0	-11.9	-8.9	*PB-00-01-14*	*14B-2B*	*1519.3*	*-11.1*	*-15.2*
PB-00-04-01	2B	1541.0	-11.3	-9.9	PB-00-02-01	1A	1519.3	-14.9	-9.2
PB-00-02-15	1A	1538.7	-12.8	-9.9	*PB-00-02-01*	*1B*	*1519.3*	*-13.6*	*-11.8*
PB-00-02-15	1B	1538.7	-13.4	-10.0	*PB-00-02-01*	*1C*	*1519.3*	*-12.3*	*-11.8*
PB-00-02-15	2A	1538.7	-13.3	-9.2	*PB-00-02-01*	*2A*	*1519.3*	*-12.6*	*-13.1*
PB-00-02-15	2B	1538.7	-13.5	-9.7	*PB-00-02-01*	*2B*	*1519.3*	*-12.9*	*-12.4*
PB-00-02-14	1A	1537.0	-13.1	-8.6	PB-00-03-24	1A	1519.3	-14.0	-8.9
PB-00-02-14	1B	1537.0	-13.6	-8.8	PB-00-03-24	1B	1519.3	-13.9	-9.2

TABLE 1 (cont.) — Carbon and oxygen isotope values of micritic carbonate from the Paleocene-Eocene boundary interval on Polecat Bench. Samples in italics were culled and not used in interpretation of $\delta^{13}C$ excursion.

Soil	Sample	Level	$\delta^{13}C$	$\delta^{18}O$	Soil	Sample	Level	$\delta^{13}C$	$\delta^{18}O$
PB-00-03-24	2A	1519.3	-14.3	-8.7	PB-00-01-06	3B	1508.0	-14.6	-8.8
PB-00-03-24	2B	1519.3	-14.9	-7.7	PB-00-01-06	4A	1508.0	-14.6	-8.8
PB-00-01-13	*1A*	*1517.8*	*-12.3*	*-11.4*	PB-00-01-06	4B	1508.0	-13.9	-8.5
PB-00-01-13	*1B*	*1517.8*	*-12.5*	*-10.4*	PB-00-03-17	1A	1507.8	-15.5	-9.2
PB-00-01-13	2A	1517.8	-14.1	-7.9	PB-00-03-17	1B	1507.8	-15.5	-9.3
PB-00-01-13	2B	1517.8	-14.0	-7.8	PB-00-03-17	2A	1507.8	-15.6	-9.3
PB-00-03-23	1A	1517.7	-14.4	-8.6	PB-00-03-17	2B	1507.8	-15.4	-9.0
PB-00-03-23	1B	1517.7	-14.3	-8.7	PB-00-03-16	1A	1507.4	-14.1	-8.2
PB-00-03-23	2A	1517.7	-13.6	-8.8	PB-00-03-16	1B	1507.4	-14.1	-7.9
PB-00-03-23	2B	1517.7	-13.5	-8.8	PB-00-03-16	2A	1507.4	-14.5	-8.5
PB-00-01-12	1A	1516.4	-13.9	-9.1	PB-00-03-16	2B	1507.4	-14.4	-8.3
PB-00-01-12	1B	1516.4	-13.8	-9.0	PB-00-01-05	1A	1507.3	-15.7	-8.7
PB-00-01-12	2A	1516.4	-14.8	-8.2	PB-00-01-05	1B	1507.3	-15.9	-8.7
PB-00-01-12	2B	1516.4	-15.2	-8.7	PB-00-01-05	2A	1507.3	-16.7	-8.9
PB-00-03-22	1A	1516.1	-12.9	-8.7	PB-00-01-05	2B	1507.3	-16.6	-8.8
PB-00-03-22	1B	1516.1	-13.8	-8.3	PB-00-01-05	3A	1507.3	-15.0	-8.4
PB-00-03-22	2A	1516.1	-13.2	-9.1	PB-00-01-05	3B	1507.3	-15.1	-8.2
PB-00-03-22	2B	1516.1	-13.7	-8.7	PB-00-01-05	4A	1507.3	-16.0	-8.1
PB-00-01-11	1A	1515.4	-13.2	-8.5	PB-00-01-05	4B	1507.3	-16.0	-8.1
PB-00-01-11	1B	1515.4	-13.3	-8.3	PB-00-03-15	1A	1506.8	-14.3	-7.9
PB-00-01-11	2A	1515.4	-13.2	-9.1	PB-00-03-15	1B	1506.8	-14.5	-7.7
PB-00-01-11	2B	1515.4	-13.0	-9.2	PB-00-03-15	2A	1506.8	-14.5	-8.2
PB-00-01-10	10A-1A	1514.3	-15.0	-7.8	PB-00-03-15	2B	1506.8	-14.2	-7.7
PB-00-01-10	10A-1B	1514.3	-14.9	-7.7	PB-00-01-04	1A	1506.5	-14.2	-9.0
PB-00-01-10	10A-2A	1514.3	-14.6	-8.1	PB-00-01-04	1B	1506.5	-14.2	-8.9
PB-00-01-10	10A-2B	1514.3	-14.5	-8.2	PB-00-01-04	2A	1506.5	-13.5	-9.0
PB-00-01-10	10B-1A	1514.1	-14.7	-7.5	PB-00-01-04	2B	1506.5	-13.6	-8.9
PB-00-01-10	10B-1B	1514.1	-14.7	-7.6	PB-00-01-03	1A	1504.9	-14.2	-8.6
PB-00-01-10	10B-2A	1514.1	-15.1	-8.0	PB-00-01-03	1B	1504.9	-14.1	-8.5
PB-00-01-10	10B-2B	1514.1	-15.0	-8.1	PB-00-03-14	1A	1504.9	-12.9	-8.6
PB-00-03-21	1A	1513.9	-15.2	-8.6	PB-00-03-14	1B	1504.9	-12.9	-8.7
PB-00-03-21	1B	1513.9	-15.2	-8.4	PB-00-03-14	2A	1504.9	-12.7	-8.0
PB-00-03-21	2A	1513.9	-15.1	-8.8	PB-00-03-14	2B	1504.9	-13.0	-8.8
PB-00-03-21	2B	1513.9	-15.2	-8.3	PB-00-01-02	1A	1502.2	-12.9	-8.2
PB-00-01-10	10C-1A	1513.6	-14.9	-8.5	PB-00-01-02	1B	1502.2	-12.5	-8.1
PB-00-01-10	10C-1B	1513.6	-15.0	-8.4	PB-00-01-02	2A	1502.2	-12.3	-8.2
PB-00-01-10	10C-2A	1513.6	-15.6	-8.9	PB-00-01-02	2B	1502.2	-12.3	-8.2
PB-00-01-10	10C-2B	1513.6	-15.7	-9.0	PB-00-01-01	1A	1500.9	-12.3	-9.1
PB-00-01-10	10D-1A	1513.2	-14.7	-7.9	PB-00-01-01	1B	1500.9	-12.3	-9.3
PB-00-01-10	10D-1B	1513.2	-14.6	-7.8	PB-00-01-01	2A	1500.9	-12.4	-9.1
PB-00-01-09	09A-1A	1512.8	-14.4	-7.8	PB-00-01-01	2B	1500.9	-12.6	-8.8
PB-00-01-09	09A-1B	1512.8	-14.5	-8.7	PB-00-03-13	1A	1500.3	-10.5	-8.9
PB-00-01-09	09A-2A	1512.8	-14.9	-8.1	PB-00-03-13	1B	1500.3	-10.2	-8.9
PB-00-01-09	09A-2B	1512.8	-15.0	-8.1	PB-00-03-13	2A	1500.3	-10.0	-8.3
PB-00-01-09	09B-1A	1512.4	-14.9	-8.6	PB-00-03-13	2B	1500.3	-10.1	-8.5
PB-00-01-09	09B-1B	1512.4	-14.8	-8.6	PB-00-03-12	1A	1499.7	-10.0	-7.9
PB-00-01-09	09B-2A	1512.4	-14.5	-8.7	PB-00-03-12	1B	1499.7	-9.9	-7.6
PB-00-01-09	09B-2B	1512.4	-14.7	-9.0	PB-00-03-12	2A	1499.7	-11.3	-8.3
PB-00-03-20	1A	1512.3	-14.9	-9.9	PB-00-03-12	2B	1499.7	-11.2	-8.3
PB-00-03-20	1B	1512.3	-14.9	-8.8	PB-00-03-11	1A	1498.5	-10.1	-9.7
PB-00-03-20	2A	1512.3	-14.9	-8.6	PB-00-03-11	1B	1498.5	-10.0	-9.7
PB-00-03-20	2B	1512.3	-14.8	-8.7	PB-00-03-11	2A	1498.5	-9.8	-9.6
PB-00-01-09	09C-1A	1512.1	-14.9	-8.8	PB-00-03-11	2B	1498.5	-9.6	-9.6
PB-00-01-09	09C-1B	1512.1	-15.1	-8.6	PB-00-03-10	1A	1495.4	-9.8	-8.7
PB-00-01-09	09C-2A	1512.1	-15.1	-8.6	PB-00-03-10	1B	1495.4	-9.4	-9.0
PB-00-01-09	09C-2B	1512.1	-15.1	-9.0	PB-00-03-10	2A	1495.4	-9.4	-7.9
PB-00-01-09	09D-1A	1511.7	-14.8	-8.2	PB-00-03-10	2B	1495.4	-9.1	-8.1
PB-00-01-09	09D-1B	1511.7	-14.4	-8.4	PB-00-03-08	1A	1494.4	-9.9	-8.9
PB-00-01-09	09D-2A	1511.7	-14.7	-8.4	PB-00-03-08	1B	1494.4	-9.9	-8.9
PB-00-01-09	09D-2B	1511.7	-14.5	-8.6	PB-00-03-08	2A	1494.4	-9.7	-9.2
PB-00-01-08	1A	1510.3	-14.3	-8.2	PB-00-03-08	2B	1494.4	-9.7	-9.4
PB-00-01-08	1B	1510.3	-14.5	-8.2	PB-00-03-07	1A	1486.0	-11.2	-9.7
PB-00-01-08	2A	1510.3	-13.3	-8.3	PB-00-03-07	1B	1486.0	-10.3	-9.9
PB-00-01-08	2B	1510.3	-13.7	-8.6	PB-00-03-07	2A	1486.0	-10.8	-9.8
PB-00-03-19	1A	1510.1	-14.0	-9.3	PB-00-03-07	2B	1486.0	-11.4	-9.8
PB-00-03-19	1B	1510.1	-14.6	-9.2	PB-00-03-06	1A	1483.4	-9.5	-9.2
PB-00-03-19	2A	1510.1	-14.6	-8.4	PB-00-03-06	1B	1483.4	-9.5	-8.8
PB-00-03-19	2B	1510.1	-14.8	-8.5	PB-00-03-06	2A	1483.4	-9.3	-9.0
PB-00-01-07.5	1A	1510.0	-13.9	-8.3	PB-00-03-06	2B	1483.4	-9.3	-9.2
PB-00-01-07.5	1B	1510.0	-13.8	-8.2	*PB-00-03-05*	*1A*	*1482.7*	*-7.2*	*-10.5*
PB-00-01-07.5	2A	1510.0	-14.7	-8.2	PB-00-03-05	1B	1482.7	-9.2	-8.9
PB-00-01-07.5	2B	1510.0	-14.7	-8.2	PB-00-03-05	1C	1482.7	-7.7	-8.2
PB-00-01-07	1A	1508.7	-14.5	-7.9	PB-00-03-05	2A	1482.7	-8.5	-9.4
PB-00-01-07	1B	1508.7	-14.7	-7.9	PB-00-03-05	2B	1482.7	-8.7	-9.4
PB-00-01-07	2A	1508.7	-14.3	-8.1	PB-00-03-04	1A	1482.0	-8.8	-9.2
PB-00-01-07	2B	1508.7	-14.0	-8.1	PB-00-03-04	1B	1482.0	-8.9	-9.3
PB-00-03-18	1A	1508.5	-13.6	-7.6	*PB-00-03-04*	*2A*	*1482.0*	*-10.0*	*-10.0*
PB-00-03-18	1B	1508.5	-13.5	-7.4	PB-00-03-04	2B	1482.0	-9.3	-8.4
PB-00-03-18	2A	1508.5	-14.1	-7.6	*PB-00-03-03*	*1A*	*1481.3*	*-11.7*	*-10.4*
PB-00-03-18	2B	1508.5	-14.3	-7.9	*PB-00-03-03*	*1B*	*1481.3*	*-11.8*	*-10.6*
PB-00-01-06	1A	1508.0	-14.2	-8.9	*PB-00-03-03*	*2A*	*1481.3*	*-13.0*	*-10.9*
PB-00-01-06	1B	1508.0	-14.2	-8.9	PB-00-03-03	2B	1481.3	-12.4	-9.1
PB-00-01-06	2A	1508.0	-14.0	-8.7	PB-00-03-02	1A	1480.8	-9.2	-9.6
PB-00-01-06	2B	1508.0	-14.0	-8.7	PB-00-03-02	2A	1480.8	-8.8	-9.6
PB-00-01-06	3A	1508.0	-14.4	-8.6	PB-00-03-02	3A	1480.8	-9.3	-9.8

characterized by markedly lower $\delta^{13}C$ values than are observed elsewhere within the section. This interval represents the Paleocene-Eocene boundary carbon isotope excursion, which is discussed in more detail below.

TABLE 2 — Measured thickness of paleosol B-horizons in the Paleocene-Eocene boundary interval on Polecat Bench.

Soil	Thickness (m)	Soil	Thickness (m)
PB-00-01-01	0.6	PB-00-03-01	0.3
PB-00-01-02	1.0	PB-00-03-02	0.2
PB-00-01-03	0.5	PB-00-03-03	0.1
PB-00-01-04	0.3	PB-00-03-04	0.6
PB-00-01-05	0.6	PB-00-03-05	0.6
PB-00-01-06	0.3	PB-00-03-06	0.6
PB-00-01-07	0.2	PB-00-03-07	0.6
PB-00-01-07.5	0.6	PB-00-03-08	0.2
PB-00-01-08	0.2	PB-00-03-09	0.3
PB-00-01-09	1.6	PB-00-03-10	0.2
PB-00-01-10	1.6	PB-00-03-11	0.2
PB-00-01-11	1.0	PB-00-03-12	0.2
PB-00-01-12	0.5	PB-00-03-13	0.3
PB-00-01-13	0.1	PB-00-03-14	0.5
PB-00-01-14	1.1	PB-00-03-15	0.3
PB-00-01-15	1.0	PB-00-03-16	0.2
PB-00-02-01	1.5	PB-00-03-17	0.2
PB-00-02-02	0.5	PB-00-03-18	0.3
PB-00-02-03	2.0	PB-00-03-19	0.5
PB-00-02-04	0.3	PB-00-03-20	1.6
PB-00-02-05	0.2	PB-00-03-21	1.6
PB-00-02-06	0.3	PB-00-03-22	0.6
PB-00-02-07	2.9	PB-00-03-23	0.5
PB-00-02-08	0.3	PB-00-03-24	0.5
PB-00-02-09	1.1	PB-00-04-01	1.4
PB-00-02-09U	0.2	PB-00-04-02	0.4
PB-00-02-10	0.2	PB-00-04-03	0.4
PB-00-02-11	0.4	PB-00-04-04	0.6
PB-00-02-12	1.0	PB-00-04-05	0.4
PB-00-02-13	0.6	PB-00-04-06	0.4
PB-00-02-14	0.2	PB-00-04-07	0.3
PB-00-02-15	0.5	PB-00-04-08	0.2
PB-00-02-16	1.5	PB-00-04-09	0.7
PB-00-02-17	0.2	PB-00-04-10	1.4
PB-00-02-18	0.1	PB-00-04-11	1.2
PB-00-02-19	0.4	PB-00-04-12	0.4
PB-00-02-20	0.3	PB-00-04-13	0.5
PB-00-02-21	0.3	PB-00-04-14	0.5
PB-00-02-22	0.5	PB-00-04-15	0.5
PB-00-02-23	1.2	PB-00-04-16	0.5

The characteristic variation of paleosol carbonate carbon and oxygen isotope compositions was investigated at several levels. The average range for $\delta^{13}C$ and $\delta^{18}O$ within individual nodules is 0.23‰ and 0.24‰, respectively ($n = 168$). Nodule averages from single sampling localities have an average range of 0.45‰ for $\delta^{13}C$ and 0.32‰ for $\delta^{18}O$ ($n = 86$). Five paleosols were sampled at multiple depths. The average range of mean carbon and oxygen isotope compositions from multiple levels within individual paleosols is 0.97‰ and 0.76‰, respectively. Additionally, four easily identifiable and laterally persistent soils were sampled in two or more local sections. The average range of mean $\delta^{13}C$ and $\delta^{18}O$ values at these laterally separated sites was 0.57‰ and 0.39‰. Overall, isotopic variability is greater at larger spatial (lateral and vertical) scales, suggesting that conditions governing the isotopic composition of the paleosol carbonate nodules were spatially variable within soils. The average range of compositions within individual paleosols, however, is minor in comparison to the temporal trends observed in our data set.

Depth to Carbonate

The paleosol B-horizons from which soil carbonates were collected varied from 10 cm to 3 m in thickness, with an average thickness of 74 cm (Table 2). These colored horizons alternate with white or gray mudstones and sandy mudstones. The contact between colored mudstones and overlying drab mudstones is often marked by an abrupt change in grain size or color, probably representing erosional truncation of the soil following soil development. In addition, these soils must undergo some post-depositional

TABLE 3 — Carbon and oxygen isotope values of paleosol carbonate spar from the Paleocene-Eocene boundary interval on Polecat Bench.

Soil	Sample	Level	$\delta^{13}C$	$\delta^{18}O$
PB-00-04-11	1SPAR	1568.2	-6.8	-16.4
PB-00-04-04	2SPAR	1549.5	-7.5	-14.7
PB-00-04-03	2SPAR	1548.4	-11.5	-13.9
PB-00-02-19	1SPAR	1545.1	-11.3	-8.6
PB-00-02-11	1SPAR	1532.2	-14.8	-15.1
PB-00-02-10	2SPAR	1531.6	-15.4	-15.5
PB-00-02-09	2SPAR	1530.5	-14.4	-14.6
PB-00-02-07	07D-1SPAR	1526.3	-13.2	-16.3
PB-00-01-12	SPAR	1516.4	-12.5	-12.5
PB-00-03-08	1SPAR	1494.4	-11.2	-9.1

compaction. Our measurements, then, provide a minimum estimate of B-horizon thickness, and place conservative bounds on total soil thickness. Nodules sampled from at least 30 cm below the top of preserved B-horizons should have formed at sufficient depth within the soils to have $\delta^{13}C$ values that are minimally affected by the penetration of atmospheric CO_2.

Where the preserved B-horizon is less than 30 cm thick (20 of the 57 soils sampled), we have no objective measure of the minimum depth beneath the soil surface at which soil carbonate formed, so atmospheric influence on the $\delta^{13}C$ value of soil carbonate is possible. To test this, we calculated average $\delta^{13}C$ values for each soil, and fit an unweighted 3-point running average to this data series. For each soil, we calculated the difference between the measured soil average $\delta^{13}C$ value and the 3-point average for that level. These differences are plotted against preserved B-horizon thickness in Figure 3. If paleosols with thin preserved B-horizons had carbonate nodules that incorporated a large amount of atmospheric carbon, nodules from these soils should be systematically enriched in carbon-13 relative to those from adjacent thicker paleosols. Least-squares regression through the data in Figure 3 produces a best-fit line with a slope of -0.045‰ per meter, which is not significantly different from zero at the 95% confidence level. We therefore conclude that, on Polecat Bench, incorporation of atmospheric CO_2 does not disproportionately affect the ^{13}C of carbonate samples from paleosols with thin preserved B-horizons.

Diagenesis

The distribution of all micrite and spar measurements in $\delta^{13}C$ vs. $\delta^{18}O$ space is non-random (Fig. 4). Micrite values cluster in two groups, one characterized by $\delta^{13}C$ values of -16‰ to -12‰ and $\delta^{18}O$ values of -9.5‰ to -7.5‰, and the other with $\delta^{13}C$ values of -10.5‰ to -8‰ and $\delta^{18}O$ values of -10‰ to -8‰. These clusters correspond to stratigraphically-distinct portions of the Polecat Bench composite section (Fig. 2), and represent P-E boundary isotope excursion values (first group) and pre- and post-excursion values (second group). Less numerous data scatter around these clusters, and it is notable that the $\delta^{18}O$ values of many of the samples are lower than those of the characteristic groups. Diagenetic spar from the carbonate nodules typically has $\delta^{18}O$ values less than -12‰, and spans a wide range of $\delta^{13}C$ values (Table 3). The inadvertent incorporation of diagenetic spar in samples of paleosol micrite is problematic, since diagenetic fluids can contribute carbon from a variety of sources and potentially obscure the paleoatmospheric record preserved in the micrite.

While mixing of carbon sources can create diagenetic carbonate with widely varying carbon isotope compositions, there is a fundamental basis for expecting that the $\delta^{18}O$ value of diagenetic carbonate will be lower than that of soil-formed micrite, and this factor can be used to distinguish altered and unaltered samples. The fractionation of oxygen isotopes during calcite precipitation is strongly temperature dependent, such that a 2° C increase in the temperature of precipitation will produce a decrease in $\delta^{18}O$ value of ca. 1‰ (Friedman and O'Neil, 1977). Diagenetic calcite formed after any substantial amount of burial, then, should be notably depleted in $\delta^{18}O$ relative to soil-formed calcite. Analyses of secondary spar from Bighorn Basin soil carbonates (Koch et al., 1995; current study), and from fossil bone (Bao et al., 1998), show that the diagenetic phase is characterized by $\delta^{18}O$ values 3‰ to 10‰ lower than co-occurring micrite that formed in the soil environment.

In several cases we see evidence that our soil micrite samples are contaminated with a component of diagenetic calcite. Samples of nodules collected from the Purple-2 marker bed of Gingerich (this volume; 1519.3 to 1519.7 m) in three local sections show obvious evidence for contamination with diagenetic calcite (Fig. 5). The samples from this soil define a line in $\delta^{13}C$ vs. $\delta^{18}O$ space, one end of which lies within the region typical for P-E boundary excursion values. The other end of

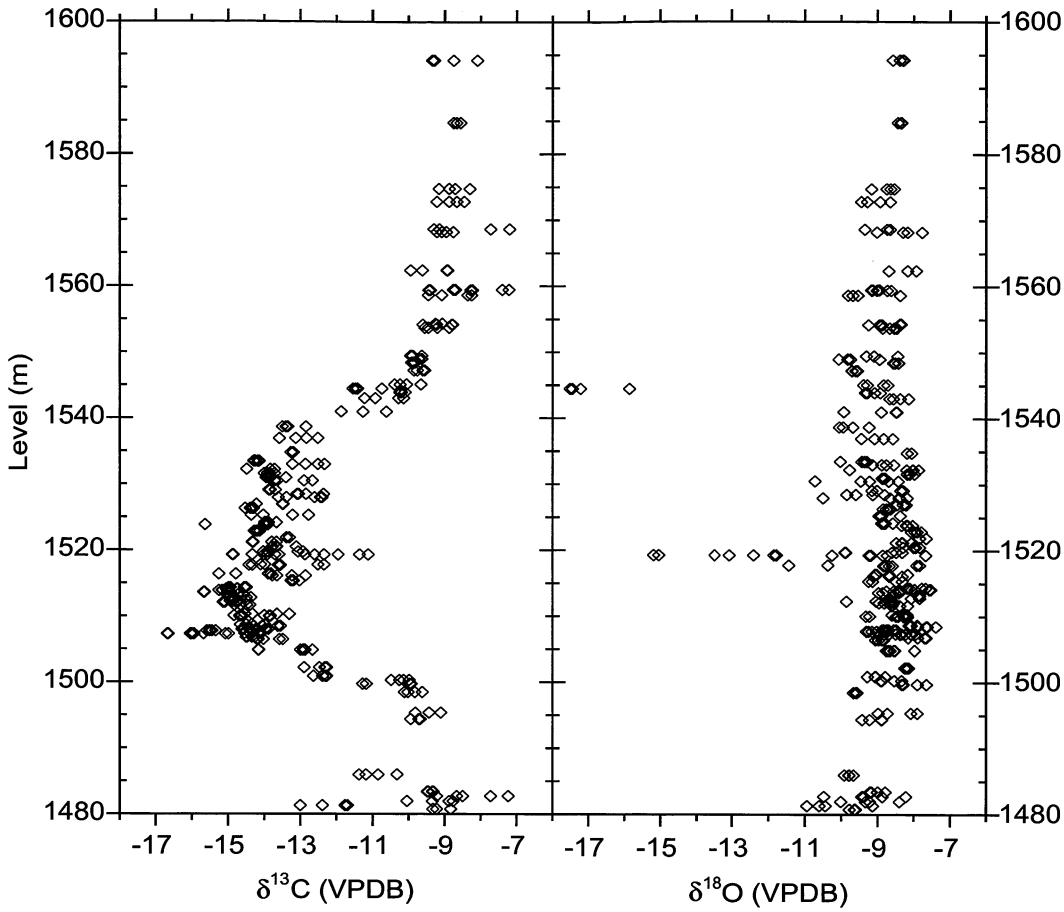

FIGURE 2 — All carbon and oxygen isotope measurements of Polecat Bench paleosol micrite plotted against stratigraphic level in the Polecat Bench composite section (Gingerich, this volume). Isotope measurements are listed in Table 1. Note fairly tight grouping (within ca. 1-3‰) of carbon and oxygen isotope values at most stratigraphic levels. Exceptions occur at the base of the section shown here, at the 1519 m level (carbon and oxygen), and at the 1544 m level (oxygen). Stratigraphic interval from 1500 m to 1540 m, with distinctly low $\delta^{13}C$ values, represents the Paleocene-Eocene boundary carbon isotope excursion.

this line lies within the broad region defined by our diagenetic spar samples, at $\delta^{13}C$ = -11‰ and $\delta^{18}O$ = -16‰ to -15‰. We suggest that physical mixing of unaltered, pedogenic micrite with a diagenetic phase produces the large range of carbon and oxygen isotope values for nodules within this particular paleosol. Although our limited analyses of diagenetic spar produced no values that can be identified directly as this hypothetical diagenetic endmember, the more extensive analyses of Bao et al. (1998) produced several values that fall near the expected range.

Given the known potential for diagenetic contamination of paleosol carbonate and the recognition that some of our measurements may reflect such contamination, we filtered the dataset to identify and remove contaminated samples from subsequent analysis. Data were filtered based on their oxygen isotope composition only, according to two criteria: (1) Individual measurements were removed if repeated analyses of the same nodule, or of nodules from the same horizon, consistently produced $\delta^{18}O$ values that were significantly (ca. 1‰ or more) different from the suspect value. (2) Multiple measurements from a single soil were excluded if they were dramatically depleted in $\delta^{18}O$ relative to nodules from surrounding soils (e.g., those data plotting outside of the "Normal Excursion Micrite" box in Fig. 5). Application of these criteria resulted in the culling of 24 of the 354 measurements in the data set (7%). Culled records are shown in italics in Table 1.

DISCUSSION

The composite carbon isotope stratigraphy spanning the Paleocene-Eocene boundary on Polecat Bench is shown in Figures 6 and 7. The first shows mean values of $\delta^{13}C$ for each paleosol in the composite section in relation to a composite

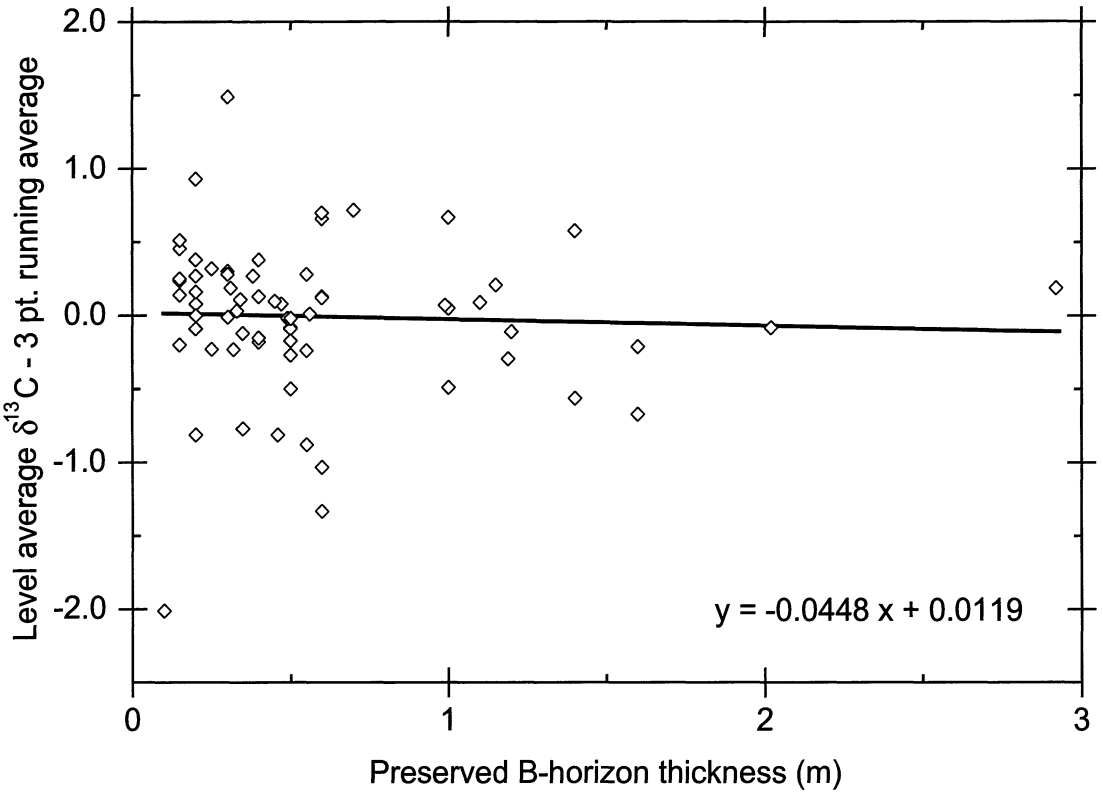

FIGURE 3 — Test for influence of atmospheric CO_2 on $\delta^{13}C$ values of paleosol carbonate sampled from thin paleosols on Polecat Bench. Differences between the mean $\delta^{13}C$ value for each soil and the unweighted 3-point average value for that level (both from Table 1) are plotted against preserved B-horizon thickness (Table 2). Least-squares regression yields a slope of -0.045‰ per meter B-horizon thickness, which is not significantly different from zero. Hence atmospheric CO_2 appears to have little effect on $\delta^{13}C$ of carbonate in paleosols with thin preserved B-horizons.

lithostratigraphic column and a detailed record of faunal change (Fig. 6), and the second shows mean values of $\delta^{13}C$ for each paleosol in each individual measured section in relation to oxygen isotope stratigraphy, a more generalized summary of faunal change, and a numerical estimate of geological age (Fig. 7). Individual measured sections are referred to by number here, with section 1 (open diamonds in Fig. 7) corresponding to the SC-343 section of Gingerich (this volume); section 2 (open squares in Fig. 7) corresponding to the SC-67 section; section 3 (open triangles in Fig. 7) corresponding to the SC-77 section; and section 4 (open circles in Fig. 7) corresponding to the SC-206 section.

The $\delta^{13}C$ Record on Polecat Bench

The most salient feature of the carbon isotope record shown in Figures 2, 6, and 7 is the negative excursion in values beginning at about the 1500 m level in the Polecat Bench composite section. Light $\delta^{13}C$ values persist for 40 m, and recovery to heavier values begins at about the 1540 m level. Carbon isotope values vary widely in the lowest 10 m of the section studied here, with low (<-10‰) values observed at two distinct levels. Carbonate nodules were scarce and carbonate horizons poorly developed in paleosols below the 1485 meter level, and a substantial number of measurements from this interval appear to be affected by diagenetic contamination (Table 1). Further sampling of this stratigraphic interval will be necessary to verify the low carbon isotope values observed here. Most paleosols below the 1500 meter level have $\delta^{13}C$ values greater than -10‰, within the range typical of pre-excursion soil carbonates (Koch et al., 1995).

Near the 1500 meter level $\delta^{13}C$ values begin to drop slightly; then they drop rapidly from -10‰ to -16‰ over a 7 m interval containing 6-7 soils. There is some suggestion here that the decrease occurs in a stepped manner, with two consecutive soils from section 1 (open diamonds in Fig. 7) producing intermediate values of about -12.5‰. This observation is consistent with previously published high-resolution marine records from ODP site 690 and 1051(Bains et al., 1999; Norris and Röhl, 1999; Bains et al., submitted). Taken together, all of the data appear

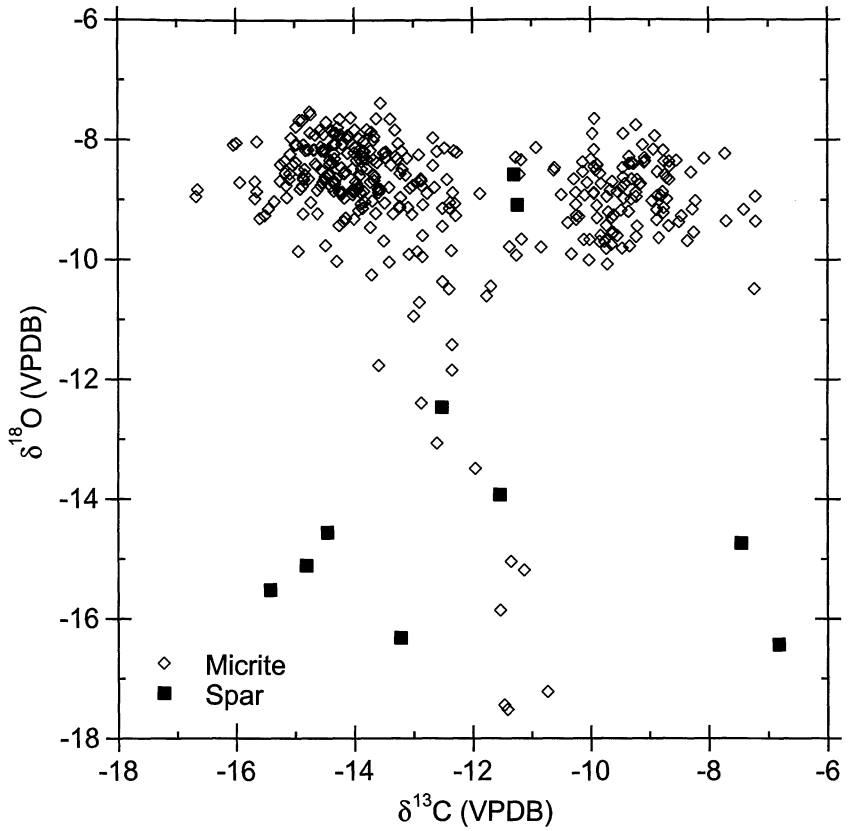

FIGURE 4 — Bivariate plot of carbon and oxygen isotope values for paleosol micrite on Polecat Bench (open diamonds; from Table 1), compared to carbon and oxygen isotope values for diagenetic spar (solid squares; Table 3). These cluster in two groups, one in the upper left quadrant (P-E boundary isotope excursion values) and one in the upper right quadrant (pre- and post-excursion values). Diagenetic spar from the carbonate nodules typically has $\delta^{18}O$ values less than -12‰, and spans a wide range of $\delta^{13}C$ values.

to indicate a stepped onset of the carbon isotope excursion, plausibly caused by multiple pulses of methane release.

The total magnitude of the $\delta^{13}C$ excursion recorded on Polecat Bench is approximately 8‰ (from pre- and post-excursion $\delta^{13}C$ values of -8‰ to minimum excursion values of -16‰), meaning that the apparent amplitude of the atmospheric excursion is at least 3.5‰ greater than the maximum value observed in proxy records for the surface ocean (Kennett and Stott, 1991). Several factors could potentially contribute to this apparent decoupling of the atmospheric and oceanic carbon reservoirs, including loss of marine records due to dissolution, changes in soil properties that control the offset between atmospheric $\delta^{13}C$ values and those of soil carbonates, or repeated addition of small quantities of methane directly to the atmosphere. The cause of the apparent decoupling is unresolved, and this should be the focus of further study.

From a minimum at 1507 m, carbon isotope values rise abruptly by ca. 2‰, and then begin to slowly and steadily increase through 30 meters of section. Superimposed on this increase are several oscillations of 2‰ or less. We have no objective method for assessing potential changes in sedimentation rates within the Polecat Bench section, and thus have no objective age model for the Polecat Bench composite section (see discussion below). However, assuming roughly uniform rates of deposition, the portion of the record from 1507 to 1540 meters is not consistent with the modeled rebound of atmospheric and oceanic $\delta^{13}C$ values following a single, massive injection of methane (Dickens et al., 1997). Again, further work is required to bring carbon cycle models and observations into agreement.

Above the 1540 meter level of the Polecat Bench composite section, $\delta^{13}C$ values of soil carbonates rise rapidly and in a roughly exponential fashion, with complete rebound to typical non-excursion values (-9‰) by 1560 meters. Samples from two local sections (sections 2 and 4) track very closely through this interval and do not show the low magnitude oscillations characteristic of the previous 33 meters of section. The pattern observed here is similar to that predicted by Dickens et al. (1997)

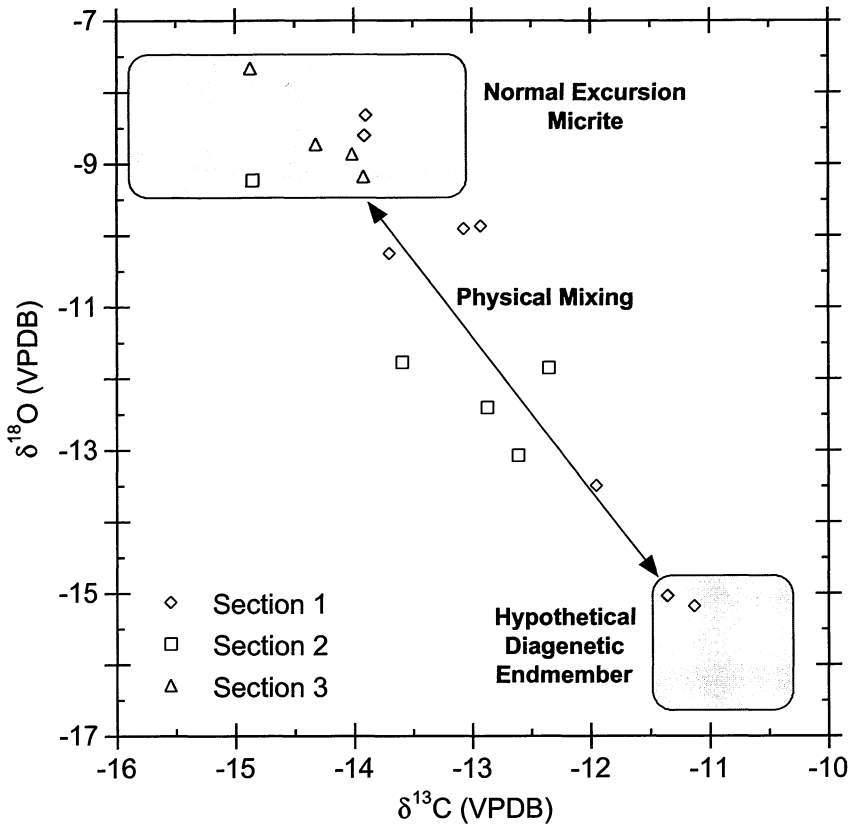

FIGURE 5 — Bivariate plot of carbon and oxygen isotope values for paleosol micritic carbonate sampled from a single soil (Purple-2: 1519.3-1519.7 m interval) in three local sections on Polecat Bench. Section 1 (open diamonds) is the SC-343 section of Gingerich (this volume); section 2 (open squares) is the SC-67 section of Gingerich (this volume); and section 3 (open triangles) is the SC-77 section of Gingerich (this volume). Isotope values define a linear array here, suggesting that these samples include an admixture in varying proportions of primary carbonate and a diagenetic phase.

for the recovery of exogenic $\delta^{13}C$ values following methane injection. Above 1560 meters the carbon isotope composition of soil carbonates remains consistent to the top of Polecat Bench.

Biotic Change in Relation to Carbon Isotope Events

The Paleocene-Eocene boundary interval on Polecat Bench is marked by a dramatic reorganization of mammalian faunas (Clyde and Gingerich, 1998). This was first recognized as a boundary between the Clarkforkian and Wasatchian land-mammal ages, at the time archaic groups like *Champsosaurus*, *Plesiadapis*, *Probathyopsis*, and *Aletodon* disappeared, and new groups including the earliest representatives of Artiodactyla, Perissodactyla, Primates, and Hyaenodontidae appeared (Rose, 1981; Gingerich, 1983). As it became better known, a fauna within the boundary interval separating latest Clarkforkian zone Cf-3 from early Wasatchian zone Wa-1was recognized to be distinctive (Gingerich, 1989). The new fauna is characterized by species of unusually small tooth and bone size, and hence small body size. The presence of *Hyracotherium* and other representatives of modern orders indicates that the fauna is Wasatchian and thus it was designated Wa-0 to reflect its stratigraphic occurrence below Wa-1 and hence its greater age. The Wa-0 fauna is found at many places in the Clarks Fork Basin and on the eastern and western margins of the Bighorn Basin (Gingerich, 1989; Strait, this volume).

Shortly afterward, a broad survey of carbon and oxygen isotopes in soil nodules and fossil mammals, spanning the entire late Paleocene and early Eocene on Polecat Bench and adjacent Clarks Fork Basin, yielded a then-surprising negative $\delta^{13}C$ spike at locality SC-67 on the end of Polecat Bench (Koch et al., 1992, 1995), enabling correlation of Wa-0 to the deep sea isotope record (Kennett and Stott, 1991) and an important benthic foraminiferal extinction event (Thomas, 1991). Initial study suggested that the base of Wa-0 is correlative with the P-E boundary isotope excursion, perhaps indicating a causal link between climatic and biotic events near the boundary (Koch et

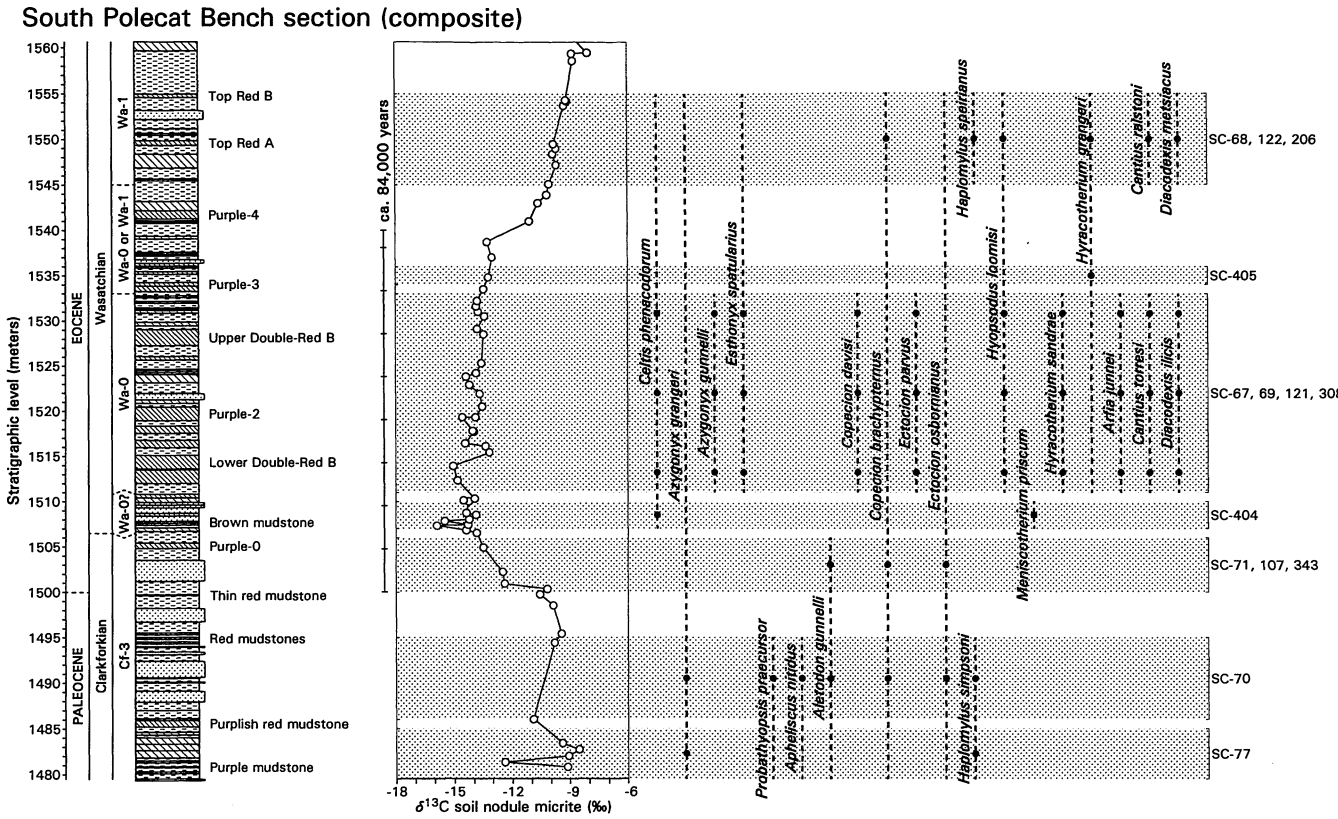

FIGURE 6 — Comparison of $\delta^{13}C$ isotope stratigraphy and biotic change at the south end of Polecat Bench. Lithostratigraphy and the ranges of *Celtis* and the principal mammalian taxa crossing the Paleocene-Eocene boundary are from Gingerich (this volume). Fourteen mammal-bearing fossil localities are known (SC-77, etc.), representing seven distinct stratigraphic intervals (shaded). These can be grouped into four time-successive associations based on their biota (Cf-3, Wa-0?, Wa-0, and Wa-1 on the ordinate). The interval labeled 'Wa-0 or Wa-1' on the ordinate is poorly-sampled and could be either Wa-0 or Wa-1 in age. The 84,000 year time scale shown here is consistent with an average rate of sediment accumulation of ca. 475 m/m.y. (Gingerich, 2000; Wing et al., 2000). Note that the beginning of the carbon isotope excursion is in the late Clarkforkian, overlapping the stratigraphic interval of localities SC-71, etc. The most negative $\delta^{13}C$ values are in the earliest zone of the Wasatchian (Wa-0?) , represented by SC-404 with the first *Celtis* and *Meniscotherium*. The remainder of the carbon isotope excursion spans the interval of the classic dwarfed Wa-0 fauna with Perissodactyla, Artiodactyla, and Primates from localities SC-67, etc. Wasatchian mammals of standard size are known from localities SC-68, etc., in zone Wa-1after carbon isotope values returned to normal (here ca. -9‰).

al., 1992). We are now able to improve this correlation by tying the Clarkforkian-Wasatchian faunal turnover directly to our new Polecat Bench carbon isotope stratigraphy.

Stratigraphic ranges for the dicot *Celtis phenacodorum* and 18 key mammalian taxa on Polecat Bench are shown in Figure 6. Specimens here were collected from 14 localities in seven successive stratigraphic intervals. The stratigraphic position of each locality and interval is well resolved, but each has a thickness (shown by stippling in Fig. 6), and fossils from a locality could have come from anywhere in the interval represented. Therefore, we take a conservative approach in representing species ranges, and show both constrained (solid circles) and unconstrained (dashed line) ranges in Figure 6. The base of a constrained range is placed in the middle of the stratigraphically lowest locality from which the taxon is known (and the opposite is true for the top of a constrained range). Localities SC-67, SC-69, SC-121, and SC-308 have been so intensively collected that we are confident that ranges of taxa found there span virtually the full thickness of the Wa-0 interval.

Probathyopsis praecursor, *Apheliscus nitidus*, *Haplomylus simpsoni*, and *Aletodon gunnelli* are characteristically Clarkforkian species (Rose, 1981) that are not present in Wa-0 or subsequent faunas. The first three may range as high as the 1495 m level, and there is a record of *A. gunnelli* between 1500 and 1506 m. Hence all three of the lower stippled intervals in Figure 6 are late Clarkforkian or Cf-3 in age.

Three specimens of *Meniscotherium priscum* are known from the Bighorn Basin, one of which was collected on Polecat Bench in 2000 from the 1507-1510 m interval. The other two

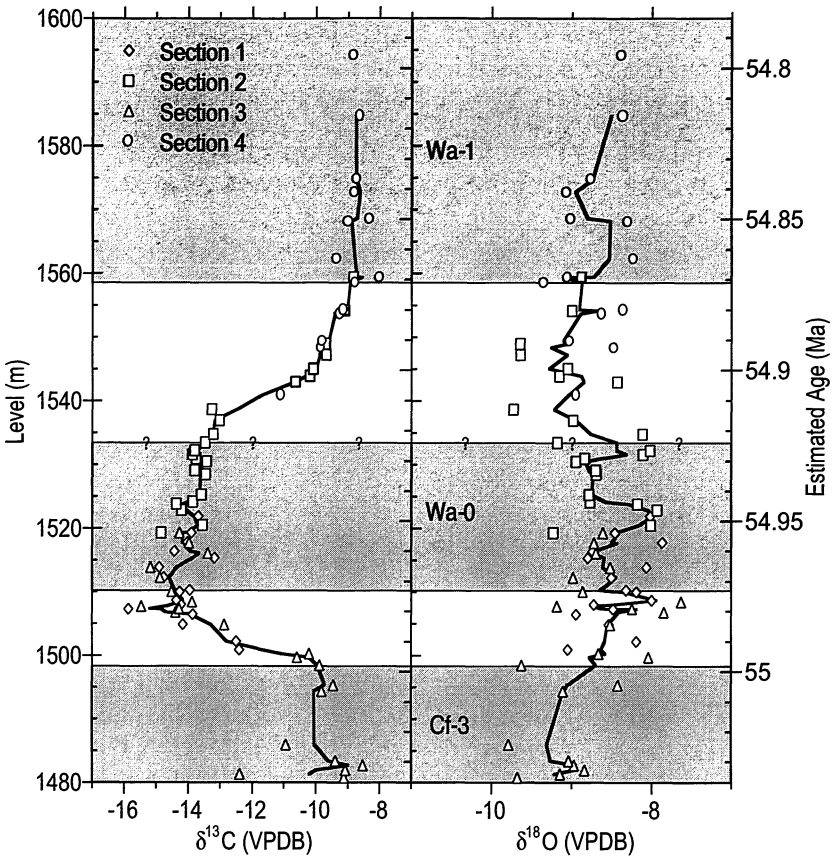

FIGURE 7 — Composite carbon and oxygen isotope records for the Polecat Bench section. Isotopic data plotted here are mean values for individual soils in each local section. Section 1 (open diamonds) = SC-343 section of Gingerich, this volume; section 2 (open squares) = SC-67; section 3 (open triangles) = SC-77 section; and section 4 (open circles) = SC-206 . Isotopic records are plotted against meter level (left scale) and estimated age (right scale, see text). Bold lines are three-point running averages for $\delta^{13}C$ and $\delta^{18}O$, respectively, with each paleosol in the composite section represented only once. Subdivisions of the Clarkforkian and Wasatchian land-mammal ages are represented by grayscale shading, interpreted conservatively (see text and Fig. 6). The lower boundary for Wa-0 is placed at 1510, above the interval containing *Meniscotherium priscum* The upper boundary for Wa-0 is placed at 1533 m, representing the upper limit of Wa-0 mammals recovered to date on Polecat Bench. Unshaded zones are intervals of faunal uncertainty that require further investigation.

specimens of *Meniscotherium priscum* both appear to be associated with a Wa-0 fauna or at least with endocarps of the dicot *Celtis phenacodorum*. Both *Meniscotherium* and *Celtis* occur in Wasatchian strata in the Bighorn Basin or elsewhere. Hence this zone is regarded as probably Wasatchian, and abbreviated Wa-0?

Faunas above the 1510 m level on Polecat Bench are dramatically different than those below and include many characteristically Eocene taxa. Wa-0 species, including *Copecion davisi*, *Ectocion parvus*, *Hyracotherium sandrae*, *Arfia junnei*, *Cantius torresi*, and *Diacodexis ilicis*, occur between 1510 and 1534 m. There is then a 10 m gap with no diagnostically Wa-0 or Wa-1 taxa. Above the 1544 m level, mammalian faunas are dominated by Wa-1 taxa, including *Haplomylus speirianus*, *Cantius ralstoni*, and *Diacodexis metsiacus*.

Constrained taxonomic ranges were used to place conservative boundaries on the Cf-3 and Wa-1 faunal zones (Fig. 7). We place the lower boundary of Wa-0 at 1510 m, and tentatively place the top of Wa-0 at 1534 m. Unshaded intervals in Figure 7 represent intervals of uncertainty within which the boundaries between the three well-established faunal zones must lie. The transition from latest Paleocene (Cf-3) to earliest Eocene (Wa-0) occurs within the stratigraphic interval marked by the initial, dramatic decline in the $\delta^{13}C$ values of paleosol

carbonates. The window of uncertainty for this faunal transition, based on the age model described below, is approximately 25 k.y. Though less well constrained, the transition between the Wa-0 and Wa-1 faunal zones appears to be correlated with the exponential rebound in carbon isotope values. The window of uncertainty for the Wa-0 to Wa-1 transition here is about 50-60 k.y. The strength of the correlations between bio- and chemostratigraphic events as they stand at present is fortunate because this will allow comparison of the relative timings of biotic transitions worldwide (e.g., Bowen et al., 2000). It is of course possible, with further work, to make the correlations on Polecat Bench even more precise.

Age Model

The age model for the Polecat Bench–Sand Coulee master section is discussed in Gingerich (2000) and Wing et al. (2000). Briefly, the bottom of magnetochron 24R, dated at 55.90 Ma (Cande and Kent, 1995), lies at the 1070 m level in the Polecat Bench composite section (Butler et al., 1981; Gingerich, this volume: fig. 3). The top of chron 24R is higher stratigraphically than we have been able to obtain reliable magnetic polarities in this section. However, the highest locality in the section, SC-295, yields *Bunophorus* representing the base of biozone Wa-5. We derived an age estimate of 53.436 Ma for the base of Wa-5 in the nearby Foster Gulch–McCullough Peaks section (Clyde et al., 1994). Interpolation between the bottom of chron 24R and the base of zone Wa-5 yields an age for the base of the Wa-0 interval (1510 m) of 54.973 Ma, an age for the top of the Wa-0 interval (1533 m) of 54.925 Ma, and a duration for the Wa-0 interval of 0.048 m.y. or 48 k.y. Our estimates for the beginning and end of the carbon isotope excursion are 54.994 Ma and 54.925 Ma, respectively, and our inferred duration for the excursion event is 84 k.y.

Alternatively, the Paleocene-Eocene carbon isotope record on Polecat Bench can be correlated with the marine bulk carbonate records from ODP site 690 (Bains et al., 1999), for which an age model has been generated using astronomical calibration (Röhl et al., 2000). The correlation of marine and terrestrial records is described in detail in Bains et al. (submitted). Here we note that the core of the $\delta^{13}C$ excursion at site 690 (from the initial drop to the level where values begin to rebound) includes four complete precessional cycles, indicating a duration of ca. 84 k.y., identical to the duration estimated here by a completely independent method.

The $\delta^{18}O$ Record on Polecat Bench

The oxygen isotope record from the Polecat Bench section is also shown in Figure 7. Trends are apparent in the time series, especially when the record is displayed as a running average, but the magnitude of these fluctuations is similar to the scatter in the data. Mean $\delta^{18}O$ values are ca. - 9.3‰ at the base of the section and increase by ca. 1‰ during the early stages of the carbon isotope excursion. Values rebound to ca. -9.3‰ by the 1540 m level and remain nearly constant or increase slightly to the top of the section. Individual measurements were separated into excursion and non-excursion groups on the basis of their $\delta^{13}C$ values (excursion samples having $\delta^{13}C < -12‰$, non-excursion samples having $\delta^{13}C > -10‰$). Mean $\delta^{18}O$ values for these two groups are -8.5‰ (n = 210) and -8.9‰ (n = 94), respectively, and results of a two-sample Student's t-test indicate that these means are significantly different at a 95% confidence level ($p < 0.0001$).

Temporal variation in the oxygen isotopic composition of Polecat Bench paleosol carbonates may reflect changes in local mean annual temperature (after Dansgaard, 1964), precipitation/evaporation ratios (e.g., Quade et al., 1989), or large-scale atmospheric circulation patterns (e.g., Amundson et al., 1996). At this time it is not possible to constrain the potential contribution of the last of these factors to the patterns in the Polecat Bench record. First order considerations suggest that significant earth surface warming during the P-E boundary interval could have induced more intense hydrological circulation, producing generally "wetter" conditions in some places on land. The resulting increase in precipitation/evaporation ratios should lead to a decrease in the $\delta^{18}O$ value of paleosol carbonate, the opposite of the trend observed in the Polecat Bench record. Assuming that the source and transport of water vapor falling over the Bighorn Basin did not change significantly during the interval marked by the carbon isotope excursion, and that the modern, spatial relationship between precipitation $\delta^{18}O$ values and mean annual temperature is applicable to temporal changes in $\delta^{18}O$ values during the P-E boundary interval, we can apply the relationship of Dansgaard (1964) to estimate temperature change in the Bighorn Basin during this interval [it is worth noting that the Dansgaard relationship is based on temperate and polar climates for the most part— the curve is not well calibrated at high temperatures (>15°C)]. Given these assumptions, the oxygen isotope record of Polecat Bench soil carbonates is consistent with a minimum of ca. 3° warming in local mean annual temperatures during the P-E boundary event.

Comparison of the faunal records to the Polecat Bench oxygen isotope record shows that the faunal zone boundaries are broadly correlative with the climatic changes reflected in the isotopic record. The Cf-3/Wa-0 boundary occurs within an interval marked by probable surface temperature warming, as indicated by increasing paleosol carbonate $\delta^{18}O$ values (Fig. 7). Previous work suggested that the first appearance of higher-order mammalian groups at the base of the Wasatchian NALMA was the result of migration across high-latitude land bridges (Gingerich, 1989), facilitated by methane-induced warming of high-latitude surface temperatures (e.g., Peters and Sloan, 2000). Our results provide strong support for such a mechanism by demonstrating the close correlation between carbon cycle, climatic, and biotic events. The transition from Wa-0 to Wa-1 faunas involved increases in species' body size (Gingerich, 1989; Clyde and Gingerich, 1998). Our record shows that this transition may also have been climate-related, as the boundary

between Wa-0 and Wa-1 faunal zones lies within or shortly following the decrease in oxygen isotope values from higher excursion values. This may indicate a cooling of local surface temperatures that favored larger body size in the derived Wa-1 species.

CONCLUSIONS

A new highly refined paleosol carbonate isotope stratigraphy across the Paleocene-Eocene boundary interval on Polecat Bench provides a detailed proxy record for the carbon isotopic composition of atmospheric CO_2. Tests of soil thickness and diagenesis were used to evaluate the reliability of the composite stratigraphy presented in Figure 7. The paleosol nodule record suggests that the $\delta^{13}C$ of atmospheric CO_2 dropped by 8‰ during this interval, and then rebounded in two steps. Details of this record may prove useful in future work addressing the causes of and response to carbon cycle perturbation at the P-E boundary, but significant questions remain regarding the partitioning of time within the Polecat Bench section and the relationship between the magnitude of the $\delta^{13}C$ shift of atmospheric CO_2 and that recorded in paleosol carbonates. Changes in the $\delta^{18}O$ of paleosol carbonates are consistent with a significant increase in local mean annual temperature during the P-E boundary event. Comparison of the timing of carbon cycle and mammalian faunal events near the P-E boundary shows that faunal transitions are coincident with major features of the carbon isotope record to within ± 10-30 k.y. Comparison of oxygen isotope and mammalian taxonomic data suggests that the diminutive forms associated with the Wa-0 faunal zone dominated an interval of increased warmth during the P-E boundary event. These species were replaced by larger taxa following the return of temperatures to near pre-boundary levels.

LITERATURE CITED

AMUNDSON, R. G., O. A. CHADWICK, C. KENDALL, Y. WANG, and M. J. DENIRO. 1996. Isotopic evidence for shifts in atmospheric circulation patterns during the late Quaternary in mid-North America. Geology, 24: 23-26.

ARENS, N. C., A. H. JAHREN, and R. AMUNDSON. 2000. Can C3 plants faithfully record the carbon isotopic composition of atmospheric carbon dioxide? Paleobiology, 26: 137-164.

BAINS, S., R. M. CORFIELD, and R. D. NORRIS. 1999. Mechanisms of climate warming at the end of the Paleocene. Science, 285: 724-727.

BAO, H., P. L. KOCH, and R. P. HEPPLE. 1998. Hematite and calcite coatings on fossil vertebrates. Journal of Sedimentary Research, 68: 727-738.

BEERLING, D. J. 2000. Increased terrestrial carbon storage across the Palaeocene-Eocene boundary. Palaeogeography, Palaeoclimatology, Palaeoecology, 161: 395-405.

BEERLING, D. J. and D. W. JOLLEY. 1998. Fossil plants record an atmospheric $^{12}CO_2$ and temperature spike across the Palaeocene-Eocene transition in NW Europe. Journal of the Geological Society of London, 155: 591-594.

BOCHERENS, H., E. M. FRIIS, A. MARIOTTI, and K. R. PEDERSEN. 1993. Carbon isotopic abundances in Mesozoic and Cenozoic fossil plants; palaeoecological implications. Lethaia, 26: 347-358.

BOWEN, G. J., P. L. KOCH, W. C. CLYDE, S. TING, Y. WANG, Y. WANG, and M. C. McKENNA. 2000. East of Eden?: temporal constraints on the appearance of 'modern' mammalian orders in Asia. Geological Society of America, Abstracts with Programs, 32: 498.

BOWN, T. M. and M. J. KRAUS. 1981. Lower Eocene alluvial Paleosols (Willwood Formation, northwest Wyoming, U.S.A.) and their significance for paleoecology, paleoclimatology, and basin analysis. Palaeogeography, Palaeoclimatology, Palaeoecology, 34: 1-30.

BOWN, T. M. and M. J. KRAUS. 1987. Integration of channel and floodplain suites. I. Developmental sequence and lateral relations of alluvial Paleosols. Journal of Sedimentary Petrology, 57: 587-601.

BOYLE, E. A. 1997. Cool tropical temperatures shift the global $d^{18}O$-T relationship: an explanation for the ice core $d^{18}O$-borehole thermometry conflict? Geophysical Research Letters, 24: 273-276.

BUTLER, R. F., P. D. GINGERICH, and E. H. LINDSAY. 1981. Magnetic polarity stratigraphy and biostratigraphy of Paleocene and lower Eocene continental deposits, Clarks Fork Basin, Wyoming. Journal of Geology, 89: 299-316.

CANDE, S. C. and D. V. KENT. 1995. Revised calibration of the geomagnetic polarity timescale for the Late Cretaceous and Cenozoic. Journal of Geophysical Research, 100: 6093-6095.

CERLING, T. E. 1984. The stable isotopic composition of modern soil carbonate and its relationship to climate. Earth and Planetary Science Letters.

CERLING, T. E., D. K. SOLOMON, J. QUADE, and J. R. BOWMAN. 1991. On the isotopic composition of carbon in soil carbon dioxide. Geochimica et Cosmochimica Acta, 55: 3403-3405.

CLYDE, W. C. and P. D. GINGERICH. 1998. Mammalian community response to the latest Paleocene thermal maximum: an isotaphonomic study in the northern Bighorn Basin, Wyoming. Geology, 261011-1014.

CLYDE, W. C., J. STAMATAKOS, and P. D. GINGERICH. 1994. Chronology of the Wasatchian land-mammal age (early Eocene) magnetostratigraphic results from the McCullough Peaks section, northern Bighorn Basin, Wyoming. Journal of Geology, 102: 367-377.

COJAN, I., M. G. MOREAU, and L. D. STOTT. 2000. Stable carbon isotope stratigraphy of the Paleogene pedogenic series of southern France as a basis for continental-marine correlation. Geology, 28: 259-262.

DANSGAARD, W. 1964. Stable isotopes in precipitation. Tellus, 16: 436-468.

DICKENS, G. R., M. M. CASTILLO, and J. C. G. WALKER. 1997. A blast of gas in the latest Paleocene; simulating first-order

effects of massive dissociation of oceanic methane hydrate. Geology, 25: 259-262.

FRICKE, H. C., W. C. CLYDE, J. R. O'NEIL, and P. D. GINGERICH. 1998. Evidence for rapid climate change in North America during the latest Paleocene thermal maximum: oxygen isotope compositions of biogenic phosphate from the Bighorn Basin (Wyoming). Earth and Planetary Science Letters, 160: 193-208.

FRICKE, H. C., and J. R. O'NEIL. 1999. The correlation between $^{18}O/^{16}O$ ratios of meteoric water and surface temperature: its use in investigating terrestrial climate change over geologic time. Earth and Planetary Science Letters, 170: 181-196.

FRIEDMAN, I., and J. R. O'NEIL. 1977. Data of geochemistry: compilation of stable isotope fractionation factors of geochemical interest. U.S. Geological Survey Professional Paper, 440KK: 1-12.

GINGERICH, P. D. 1983. Paleocene-Eocene faunal zones and a preliminary analysis of Laramide structure deformation in the Clarks Fork Basin, Wyoming. Wyoming Geological Association Guide Book, 34: 185-195.

GINGERICH, P. D. 1989. New earliest Wasatchian mammalian fauna from the Eocene of Northwestern Wyoming: Composition and diversity in a rarely sampled high-flood plain assemblage. University of Michigan Papers on Paleontology, 28: 1-97.

GINGERICH, P. D. 2000. Paleocene-Eocene boundary and continental vertebrate faunas of Europe and North America. *In* B. Schmitz, B. Sundquist, and F. P. Andreasson (eds.), Early Paleogene Warm Climates and Biosphere Dynamics, GFF [Geologiska Föreningens Förhandlingar], Geological Society of Sweden, Uppsala, 122: 57-59.

KATZ, M. E., D. K. PAK, G. R. DICKENS, and K. G. MILLER. 1999. The source and fate of massive carbon input during the latest Paleocene thermal maximum. Science, 286: 1531-1533.

KENNETT, J. P. and L. D. STOTT. 1991. Abrupt deep-sea warming, palaeoceanographic changes and benthic extinctions at the end of the Palaeocene. Nature, 353: 225-229.

KOCH, P. L., J. C. ZACHOS, and D. L. DETTMAN. 1995. Stable isotope stratigraphy and paleoclimatology of the Paleogene Bighorn Basin (Wyoming, USA). Palaeogeography, Palaeoclimatology, Palaeoecology, 115: 61-89.

KOCH, P. L., J. C. ZACHOS, and P. D. GINGERICH. 1992. Correlation between isotope records in marine and continental carbon reservoirs near the Palaeocene-Eocene boundary. Nature, 358: 319-322.

KRAUS, M. J. 1987. Integration of channel and floodplain suites. II. Vertical relations of alluvial Paleosols. Journal of Sedimentary Petrology, 57: 602-612.

NORRIS, R. D. and U. RÖHL. 1999. Carbon cycling and chronology of climate warming during the Paleocene-Eocene transition. Nature, 401: 775-778.

PETERS, R. B. and SLOAN, L.C. 2000. High concentrations of greenhouse gases and polar stratospheric clouds: a possible solution to high-latitude faunal migration at the latest Paleocene thermal maximum. Geology, 28: 979-982.

QUADE, J., T. E. CERLING, and J. R. BOWMAN. 1989. Systematic variations in the carbon and oxygen isotopic composition of pedogenic carbonate along elevation transects in the southern Great Basin, United States. Geological Society of America Bulletin, 101: 464-475.

RÖHL, U., T. J. BRALOWER, R. D. NORRIS, and G. WEFER. 2000. New chronology for the late Paleocene thermal maximum and its environmental implications. Geology, 28: 927-930.

ROSE, K. D. 1981. The Clarkforkian land-mammal age and mammalian faunal composition across the Paleocene-Eocene boundary. University of Michigan Papers on Paleontology, 26: 1-197.

THOMAS, E. 1991. The latest Paleocene mass extinction of deep sea benthic foraminifera: result of global climate change. Geological Society of America Abstracts with Programs, 23: A141.

WING, S. L., H. BAO, and P. L. KOCH. 2000. An early Eocene cool period? Evidence for continental cooling during the warmest part of the Cenozoic. *In:* B. T. Huber, K. G. Macleod, and S. L. Wing (eds.), Warm Climates in Earth History. Cambridge University Press, Cambridge, UK, pp. 197-237.

ZACHOS, J. C., K. C. LOHMANN, J. C. G. WALKER, and S. W. WISE. 1993. Abrupt climate changes and transient climates during the Paleogene: a marine perspective. Journal of Geology, 101: 191-213.